A linear sensorimotor transformation accounts for response range-dependent biases in human heading estimation

Qi Sun[1,2,3*†], Ling-Hao Xu[4†], Alan A Stocker[5*]

[1] School of Psychology, Zhejiang Normal University, Jinhua, China, PRC

[2] Intelligent Laboratory of Zhejiang Province in Mental Health and Crisis Intervention for Children and Adolescents, Jinhua, P. R. China

[3] Key Laboratory of Intelligent Education Technology and Application of Zhejiang Province, Zhejiang Normal University, Jinhua, P. R. China

[4] Dominick P. Purpura Department of Neuroscience, Albert Einstein College of Medicine, Bronx, New York, USA

[5] Department of Psychology, University of Pennsylvania, Philadelphia, Pennsylvania, USA.

[†] **Co-first authors**

*** Correspondence:**

SQ: sunqi_psy@zjnu.edu.cn; https://orcid.org/0000-0001-9382-3249

AS: astocker@psych.upenn.edu, https://orcid.org/0000-0002-2041-1515

Abstract

Accurate estimation of heading direction from optic flow is a crucial aspect of human spatial perception. Previous studies have shown that humans are typically biased in their estimates of heading directions, but the reported results are inconsistent. While some studies found that humans generally underestimate heading direction (central bias), others find the opposite, an overestimation of heading direction (peripheral bias). We conducted three psychophysical experiments showing that these conflicting findings do not reflect inherent differences in heading perception. Rather we found that they are caused by the different sizes of the response range that participants were allowed to utilize when reporting their estimates. Notably, we show that participants' heading estimates monotonically scale with the size of the response range, leading to underestimation for small and overestimation for large response ranges. Additionally, neither the speed profile of the optic flow pattern nor the response method (mouse vs. keyboard) significantly affected participants' estimates.

Furthermore, we derived a Bayesian observer model to quantitatively account for participants' estimation behavior. The model assumes an efficient sensory encoding of heading direction according to the natural prior of freely behaving humans. In addition, the model incorporates a motor stage that linearly maps the percept to the reported estimate with a scaling factor that depends on the size of the response range. This perception-action model accurately predicts participants' estimates both in terms of mean and variance. Our findings underscore that human heading perception follows efficient Bayesian inference; differences in participants reported estimates can be solely attributed to differences in linear mapping from percept to probe response.

Introduction

An accurate and precise estimation of stimulus features based on visual information is important for a successful interaction with our environment. However, humans are often biased in their estimates of stimulus features. For instance, orientations are often inaccurately perceived, a phenomenon referred to as the oblique effect [1], while color estimates exhibit systematic compressions towards the center of individual color categories [2]. Most of these biases are robust and have been successfully replicated across multiple studies performed by different labs. For example, the effect that perceived visual orientations are typically biased away from cardinal orientations (the aforementioned oblique illusion), is robust and has been repeatedly reported with little quantitative difference [3-5]. However, that is not true for biases in perceived heading direction (i.e., self-motion direction) based on optic flow (Fig. 1a, S1 and S2 for Movies). Some studies found that participants consistently overestimated their heading direction, thus exhibiting a peripheral bias [6-8]. Whereas in other studies, participants consistently underestimated their heading direction, producing a consistent center bias towards the straight-ahead direction [9-15]. What contributes to these seemingly contradictory results remains unclear, in particular since all these studies use very similar optic flow stimuli in overall very similar experiments. A careful examination of the differences in experimental design between these studies, however, revealed two potential factors that may have caused the contrasting behavioral results. The first factor concerns the **speed profiles** of the used optic flow stimuli. Studies that found central biases (underestimation) generally utilized optic flow patterns that simulate observers moving in 3D space at constant speed [10-12, 15]. In contrast, studies that reported a peripheral bias (overestimation) typically employed optic flow patterns that simulate observer moving at variable speeds [6-8, 16]. The second factor is the **response method**. Specifically, in the studies that

reported central bias, participants expressed their perceived headings by adjusting the position of a probe along a horizontal line using the mouse (see right panel in Fig. 1b; [10-12, 15]), whereas in the studies that reported peripheral bias, participants adjusted the position of a probe on a circle using key presses (see middle panel in Fig. 1b; [6, 7]). It is unclear in what way these two factors are responsible for the different type of bias and why.

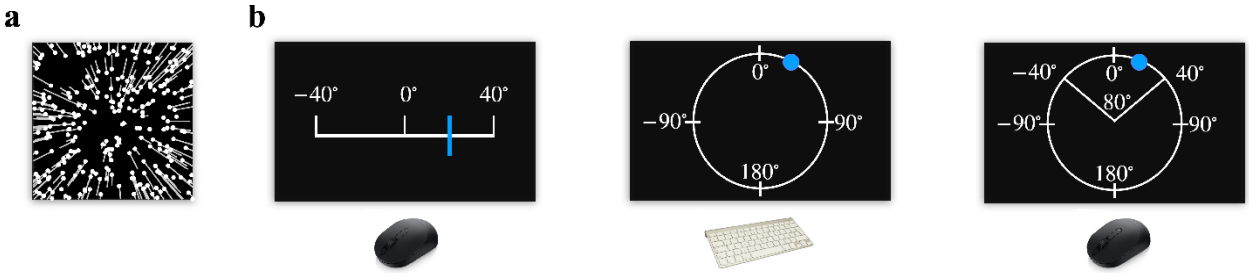

Fig. 1. Heading estimation based on optic flow. (a) Illustration of an optic flow pattern [17] that simulates an observer moving straight-forward (i.e., a heading direction of 0°). The dots indicate the positions of dots in the first frame. The white lines (invisible in the experiment) indicate the motion trajectory of dots in the subsequent frames. Previous studies have used very similar flow stimuli to investigate heading perception. (b) Response methods used in our three experiments. In Experiment 1, participants either used a mouse-controlled probe on a horizontal line with a range of 80° (left panel) or moved a key-controlled dot on a circle with a range of 360° (middle panel) to indicate their perceived heading direction. In Experiment 2, all participants reported their perceived heading direction by moving a mouse-controlled probe on a line (block 1), circle (block 2), or an arc with a range of 80° (block 3). In Experiment 3, participants reported their estimates for three different arc ranges: 80°, 160°, or 240°. The numbers denoting the range or degrees were not visible to participants during the experiment.

Supporting information S1 and S2 Movies provide examples of the optic flow stimuli used in the experiments, demonstrating constant and variable speed profiles, respectively.

In the current study, we undertook three experiments aimed at determining how stimulus speed profiles and response ranges may affect heading estimates based on optic flow. Our findings reveal a gradual transition from underestimation to overestimation biases with increasing response range, establishing that the response range played a pivotal role in causing distinct estimation biases. Building on these empirical results, we introduce a model that extends the efficient Bayesian observer model of Wei & Stocker [18-20]. The extended observer model assumes that perceived heading direction is linearly mapped to participants' reported estimates with a scaling factor that grows monotonically with the size of the response range. Importantly, our model accurately predicts both biases and variances in participants' heading estimates across different response ranges, suggesting that divergent heading estimates can be attributed exclusively to variations in response ranges. This novel extension of the efficient Bayesian observer model provides a comprehensive explanation for the observed biases in heading estimation and highlights the importance of considering motor mapping in perceptual decision-making tasks.

Materials and Methods

Experimental methods

Participants

All participants were enrolled in Zhejiang Normal University. All were naive to the experimental purpose with normal or corrected-to-normal vision. The experiment was approved by the Scientific and Ethical Review Committee in the Department of Psychology of Zhejiang Normal University. Thirty-six participants took part in Experiment 1 and were randomly divided into two groups (Group 1: 11 females, 7 males, 19-28 years; Group 2: 11 females, 7 males, 20-25 years). Eighteen participants took part in Experiment 2 (10 females, 8 males; 19-27 years). Another eighteen participants took part in Experiment 3 (9 females, 9 males; 17-23 years).

Apparatus

The experiment was programmed in MATLAB using the Psychophysics Toolbox 3 and presented on a 27-inch Dell monitor (resolution: 2560 H× 1440 V pixels; refresh rate: 60 Hz) with NVIDIA GeForce GTX 1660Ti graphics card.

Stimuli

The optic flow stimuli (80° H × 80° V visual angle, Fig. 1a) simulated observers translating in a 3D dot-cloud (depth range: 0.20 – 5 m; eye-height: 0.17 m) consisting of 126 dots (diameter: 0.2°). The simulated self-motion speed was either constant (i.e., 1.5 m/s, used in Experiments 1-3; see Supplementary materials: Movie 1), or first accelerating (0 m/s to 3 m/s) and then decelerating to 0 m/s (used in Experiment 1; see Supplementary materials: Movie 2). Acceleration and deceleration were identical in magnitude (12 m/s^2). Two types of speed profiles generated the same moving distances (0.75 m) during the stimulus presentation. The simulated self-motion direction (i.e., heading) was selected from ±3°, ±9°, ±15°, ±21°, ±27°, and ±33°. Negative and positive values denote the headings left (-) or right (+) to the straight-ahead direction (0°).

Procedure

Participants sat in a dark room with their heads stabilized with a chin-rest. They viewed the display binocularly with a 20-cm viewing distance. During the experiment, participants were asked to fixate on the display center without head and body movements during the entire experiment duration. Straight-ahead direction was aligned with the display center.

The trial procedures were the same across all three experiments. Each trial started with a heading display for 500 ms, followed by participants' responses (self-timed). The next trial started right after a participant's response. Heading direction in each trial was randomly selected from ±3°, ±9°, ±15°, ±21°, ±27°, and ±33°.

Experiment 1 used a mixed experimental design. Response methods (line vs. circle responses) were the between-subject variable, while speed profiles (constant vs. variable speeds) were the within-subject variable. Thus, the current experiment included four conditions. Note that, in the line-response condition, the left and right end-points of the line were shifted from the display center (0°) by 40°, resulting in a response range of 80° (left panel in Fig. 1a). Participants used the mouse to adjust the probe position on the line to indicate their heading estimates. In contrast, in the circle-response condition, participants could freely adjust the probe position on a circle, resulting in a response range of 360° (middle panel in Fig. 1a). Participants reported their heading estimates by pressing the arrow keys to adjust the probe dot position on the circle. The two speed profiles were tested in two separate blocks. That is, in the line- or circle-response conditions, participants completed two blocks. Each block corresponded to one speed profile. In each block of the line- and circle-response conditions, every heading direction was repeated 40 and 15 times, leading to a total of 480 and 180 trials, respectively. There were fewer trials in the circle-response condition than in the line-response condition because participants typically took more time to respond in the circle condition. The sequence of the two blocks in the line- and circle-response conditions was counterbalanced among participants. For example, one participant would first finish the block with the constant speed, followed by the block with the variable speed; another participant would first finish the block with the variable speed, followed by the constant speed.

Experiment 2 was similar to Experiment 1, except that **i)** the motion speed was always constant, **ii)** the probe on the line or circle was controlled only by the mouse, and **iii)** each participant in the current experiment finished three blocks of trials. Each block corresponded to one response method (e.g., line, arc, or circle) and consisted of 240 trials (20 trials × 12 headings).

The response range for the arc condition was 80° (right panel in Fig. 1a). The conducting sequence of the three blocks was counterbalanced among participants.

Experiment 3 was similar to Experiment 2, except that only one block was conducted. The block contained 12 heading directions and three response range conditions: 80°, 160°, and 240°. There was a total of 36 combinations. Each combination was repeated 15 times, resulting in 720 trials. All trials were randomly interleaved.

Before starting the experiment, participants were given 20 practice trials in which the speed profile was constant. The practice trials helped participants to familiarize the stimuli and response methods. After the practice part, the experiment started.

Modeling methods

Our model consists of two parts: the efficient Bayesian observer model as originally proposed (Fig. 3a, [19, 20]) and a linear perception-action mapping stage (Fig. 4b).

Part 1: the efficient Bayesian observer model

The efficient Bayesian observer model was built based on the following three assumptions:

(1) The neural system encodes stimulus features (e.g., heading direction from optic flow) efficiently, following the efficient coding hypothesis [21, 22];

(2) The sensory noise follows a von-Mises distribution in sensory space. Because the noise is homogeneous in this space (see below), the likelihood function $p(m|\theta)$ for a stimulus θ_0 also follows a von-Mises distribution, where μ is the distribution mean equal to $F(\theta_0)$, and κ is the concentration parameter that represents the sensory noise magnitude;

(3) Following assumption (1) and [20], the prior distribution $p(\theta)$ is inversely proportional to the discrimination threshold $D(\theta)$, thus

$$p(\theta) \propto \frac{1}{D(\theta)} \tag{1}$$

In the current study, we used the visual discrimination data from [8] and fitted a bimodal Von-Mises distribution to obtain a smooth approximation of the prior distribution (Fig. 4c).

With the above assumptions, we provide the following step-by-step formulation of the extended efficient Bayesian observer model:

1.1 Encoding and Mapping Function $F(\theta)$

To encode the heading direction, we employed a one-to-one mapping to transform the heading direction θ from stimulus space into sensory space according to efficient coding, given by

$$F(\theta)=\int_{-\pi}^{\theta} p(\vartheta)\, d\vartheta \tag{2}$$

which represents the cumulative prior distribution $p(\theta)$ with θ in $[-\pi,\pi)$.

1.2 Sensory measurement m

For each heading direction θ_0, the corresponding measurement on the sensory space m is given by,

$$m=F(\theta_0) + \eta \tag{3}$$

where η represents the internal sensory noise.

1.3 Likelihood Function $p(m|\theta)$

We assume the sensory noise η follows a von-Mises distribution in the sensory space:

$$p(m|\theta)=\frac{1}{2\pi I_0(\kappa)} e^{(\kappa\, cos(m - F(\theta)))} \tag{4}$$

where $I_0(\cdot)$ is the modified Bessel function of order 0, and κ is the concentration parameter that controls the noise magnitude. The likelihood function $p(m|\theta)$ captures the bottom-up sensory information for a specific measurement m.

1.4 Prior Distribution $p(\theta)$

The prior distribution $p(\theta)$ represents the observer's belief about the probability of each heading direction θ before any sensory observation. As stated in assumption (3), we assume it to be

inversely proportional to the heading discrimination threshold $D(\theta)$ measured in the experiment [8]. We keep this prior distribution fixed for all model fits and predictions of our model analysis.

1.5 Posterior Distribution $p(\theta|m)$

With the likelihood function $p(m|\theta)$ and the prior distribution $p(\theta)$ defined above, the posterior distribution $p(\theta|m)$ can be computed using Bayes' rule:

$$p(\theta|m) \propto p(m|\theta)\, p(\theta) \tag{5}$$

1.6 Bayesian Estimate $\hat{\theta}(m)$

To obtain the Bayesian estimate $\hat{\theta}(m)$ for a given measurement m, we minimize the expected loss based on a specific loss function $L(\hat{\theta}, \theta)$:

$$\theta(m) = \underset{\theta}{argmin} \int L(\hat{\theta},\theta)\, p(\theta|m)\, d\theta \tag{6}$$

For the squared error loss function (L_2 norm: $L(\hat{\theta}, \theta)=\|\hat{\theta}-\theta\|_2$), the Bayesian estimate is the mean of the posterior distribution:

$$\hat{\theta}(m) = \int \theta\, p(\theta|m)\, d\theta \tag{7}$$

1.7 Estimation Bias $b(\theta_0)$ and Standard Deviation $\sigma(\theta_0)$

The expected bias $b(\theta_0)$ for a given stimulus value θ_0 can be computed by marginalizing the estimate $\hat{\theta}(m)$ over the measurement distribution $p(m|\theta_0)$:

$$b(\theta_0) = \int \hat{\theta}(m)\, p(m|\theta_0)\, dm - \theta_0 \tag{8}$$

To compute the standard deviation of the circular variable $\hat{\theta}$, we first calculate the average cosine and sine of the estimate:

$$\begin{aligned} C(\theta_0) &= \int cos\left(\hat{\theta}(m)\right) p(m|\theta_0)\, dm \\ S(\theta_0) &= \int sin\left(\hat{\theta}(m)\right) p(m|\theta_0)\, dm \end{aligned} \tag{9}$$

Then, the circular standard deviation $\sigma(\theta_0)$ of the estimate for a given stimulus value θ_0 can be computed as:

$$\sigma(\theta_0) = \sqrt{2(1-\sqrt{C(\theta_0)^2+S(\theta_0)^2})} \tag{10}$$

Part 2: Linear Perception-Action Mapping

To account for the effect of the response range on the reported heading estimates, we extend the efficient Bayesian observer model by introducing a linear mapping between the perceived heading direction $\hat{\theta}(m)$ and the reported heading estimate $\hat{\theta}_r(m)$:

$$\hat{\theta}_r(m) = \alpha_i\, \hat{\theta}(m) \tag{11}$$

where α_i (i = 1, 2, 3) is a scaling factor that depends on the response range condition (Fig. 5a).

Part 3: Model Fitting

Our extended model has four free parameters: the sensory noise magnitude κ (assumed to be constant across response range conditions) and the three scaling factors $\{\alpha_1, \alpha_2, \alpha_3\}$(one for each response range condition). We jointly fit these parameters to the data from all participants in Experiment 3 using maximum likelihood estimation:

$$\{\kappa^*, \alpha_1^*, \alpha_2^*, \alpha_3^*\} = \underset{\kappa,\alpha_1,\alpha_2,\alpha_3}{argmax}\, p(X|\kappa,\alpha_1,\alpha_2,\alpha_3) \tag{12}$$

where X represents the observed heading estimates across all participants and conditions.

Experimental Results

Impact of navigation speed on reported heading direction (Experiment 1)

Thirty-six participants were exposed to two optic flow displays generated by simulated movement of observers in a 3D dot-cloud environment: movement was either at constant speed or at variable speed (S1 and S1 for Movies 1 and 2). Participants were exposed to heading directions within the

range [-33°, 33°] with uniform sampling at 6° steps. Negative and positive values denote the headings left (-) or right (+) of straight-ahead direction (0°). Consistent with previous studies, one group of participants (N=18) reproduced their perceived heading directions by moving a mouse-controlled probe on a horizontal line with a limited response range (80°, left panel in Fig. 1b), while another group adjusted a key-controlled dot on a circle (response range is 360°, middle panel in Fig. 1b; see Methods for more details). No feedback was given to participants.

Fig. 2 illustrates the bias (difference between the average heading estimate and the actual heading direction) and the standard deviation of subjects' estimates for the two different speed and response conditions. The bias patterns are similar for the two speed profiles but exhibit significant differences for the two response methods. Specifically, participants overestimated heading direction (peripheral bias) when reporting their estimates on the circle (red line), whereas they underestimated heading direction (central bias) when reporting on the line (black line). These results suggest that the speed pattern by which participants navigate does not affect perceived heading directions. Using different response methods, however, can substantially affect the reported heading estimates.

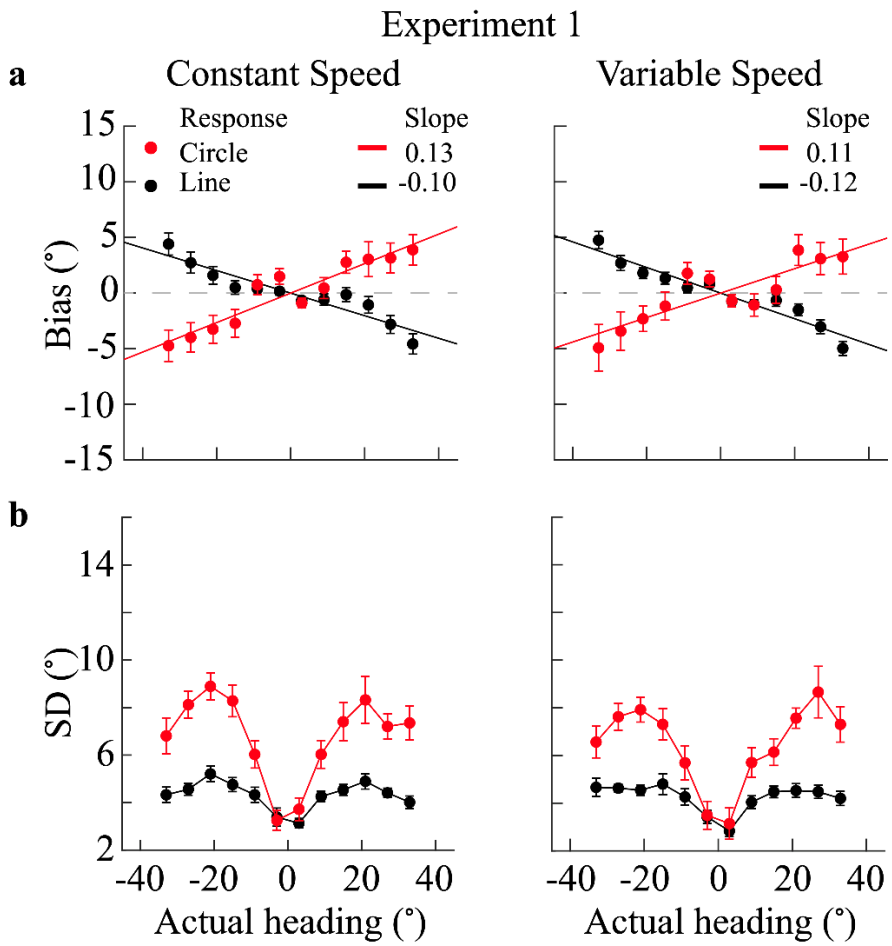

Fig. 2. Bias and standard deviation in perceived heading direction (Experiment 1, N=18) (a) Average bias of participants as function of actual heading angle (0° corresponds to straight-ahead). To capture its overall trend, we fit a linear function to the measured bias curves (solid lines). Positive slope values indicate overestimation (peripheral bias), while a negative slope indicates underestimation (central bias). (b) Average standard deviation (SD) of heading estimates across participants as a function of actual heading direction. Red dots represent estimates reported on the circle, and black dots represent estimates reported on the line. Error bars in all plots indicate the standard error across participants.

Likewise, variability in participants' estimates also depends on the response method but not the speed profile. Standard deviations were significantly larger in the circle response condition compared to the line response condition, although the overall pattern was similar (Fig. 2b).

Impact of response method (mouse vs. keys) on reported heading direction (Experiment 2)

Experiment 2 was identical to Experiment 1, with the exceptions that **i)** the optic flow displays were simulated assuming an observer moving at a constant speed, and **ii)** participants reported their perceived heading direction by adjusting a cursor with a computer mouse. In addition to the line- and circle-response conditions (left and middle panels in Fig. 1b), we also included an arc-response condition where participants reported their heading direction on an 80° response arc ([-40°, +40°] range; right panel in Fig. 1b). Note that the tested heading directions never exceeded a range of [-33°, 33°]. The three response conditions were randomly interleaved in the experiment (see Methods for details).

Fig. 3a shows the average biases across all 18 participants in Experiment 2. Participants clearly underestimate heading direction when reporting their estimates both on the 80° line and the 80° arc. Note, the biases are not significantly different between the two conditions. In contrast, participants clearly overestimated heading directions in trials where they reported their estimates on the circle. Consistent with the data from Experiment 1, the standard deviation of participants' estimates was significantly larger in the circle response conditions than in the line and arc response conditions (Fig. 3c); again, there was no significant difference between the latter two conditions. Results of Experiment 2 indicate that the divergent bias patterns are solely due to a difference in response range (80° arc vs. full circle). The difference in response method had no effect on participants' reported heading direction.

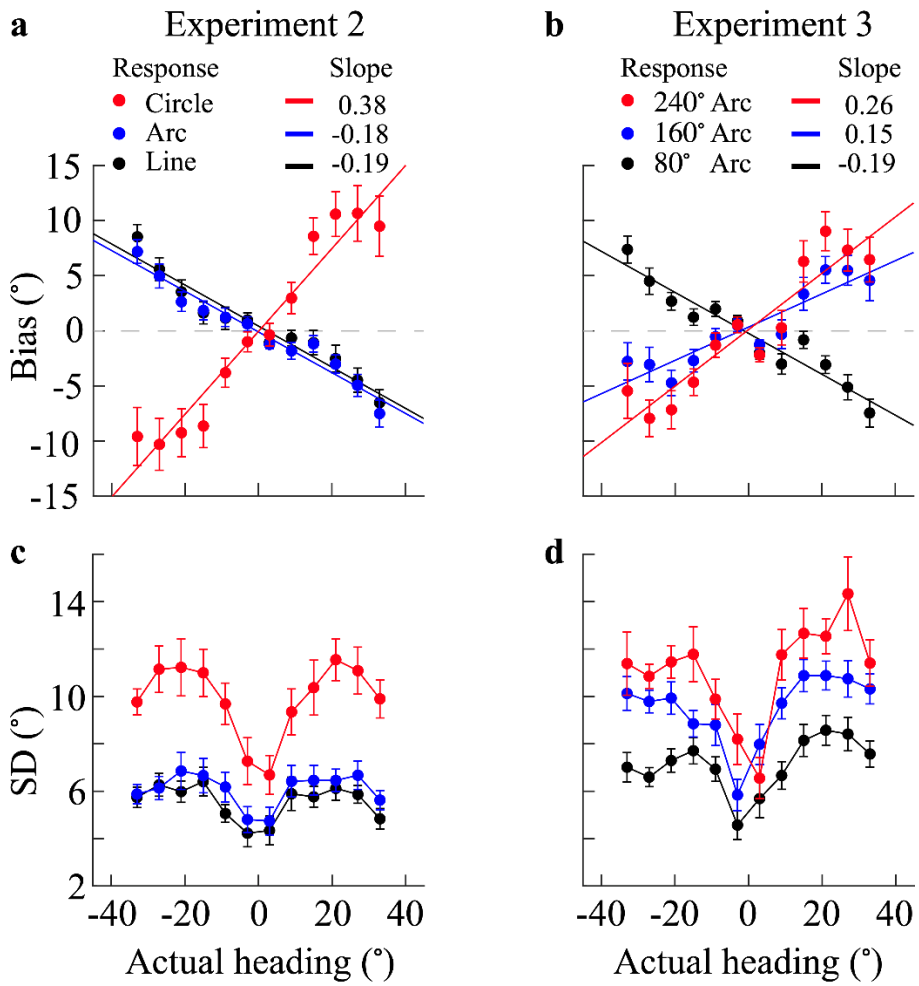

Fig. 3. Bias and standard deviation in perceived heading direction (Experiments 2 and 3, N=18) (a, b) Average bias of participants (N=18) as a function of heading direction (0° corresponds to straight-ahead). Solid lines represent linear fits to the average bias curves. A positive slope indicates overestimation (peripheral bias), while a negative slope indicates underestimation (central bias). (c-d) Average standard deviation of heading estimates as a function of heading direction. In (a, c), the red, blue and black dots represent the circle, 80° arc, and line response conditions, respectively. In (b, d), the red, blue and black dots represent the 240°, 160°, and 80° arc response conditions, respectively. In all panels, error bars indicate the standard errors across participants.

Impact of response range on reported heading direction (Experiment 3)

Results of Experiment 2 indicate that heading estimates may progressively increase when participants are provided with an increasingly larger response range. We recruited another 18 participants to conduct Experiment 3, in which the response range was progressively increased (i.e., arcs of 80°, 160°, and 240°). The experimental design was similar to that of Experiment 2 (see Methods for more details). Importantly, trials of the different range conditions were randomly interleaved. Fig. 3b shows that participants central bias (underestimation) is progressively reduced with increasing response range, eventually turning into a peripheral bias (overestimation) when the response range is 240° or more. Standard deviations of participants' estimates as a function of actual heading direction are similar in shape across all response conditions but progressively increase with increasing response range (Fig. 3d). The results of Experiment 3 further confirm that the response range is the main factor leading to different estimation biases.

In summary, the results from the three experiments demonstrate that participants' heading estimates were neither significantly different between different speed profiles (constant vs. variable) nor did they depend on the response method used. However, estimates were strongly dependent on the response range, showing progressively increasing biases from underestimation to overestimation with increasing size of the response range. The difference in response range is the main explanation for the previously reported, contrasting biases in human heading estimation.

Bayesian Observer Model

Bayesian observer models express how knowledge about the distribution of a stimulus feature (i.e., the prior) needs to be combined with current sensory information (i.e., the likelihood) in order to optimally estimate the value of the feature [23-25]. Measured heading direction distributions by freely behaving human observers show a characteristic peak for straight-ahead heading [26]. With

317 such a prior, however, standard Bayesian observer models consistently predict a bias toward the
318 prior peak, thus a central bias toward straight-ahead direction [10-12, 15]. As a result, these models
319 cannot account for peripheral biases. More importantly, previous formulations of the Bayesian
320 observer model did not incorporate aspects of motor planning and mapping, and thus are generally
321 not equipped to explain the dependency on the response range we found in our experiments.

322 Here, we present a Bayesian observer model that can account for these range effects. The
323 model extends the Bayesian observer model constrained by efficient coding proposed by Wei and
324 Stocker [18-20]. The original model's innovation was to integrate efficient coding theory [21, 22]
325 with a Bayesian observer model, resulting in a unified framework known as the efficient Bayesian
326 observer model. The model assumes that the neural system efficiently encodes the stimulus by
327 maximizing the mutual information between the stimulus and its sensory representation.
328 Subsequently, guided by the observer's prior belief $p(\theta)$, the efficient sensory representation is
329 optimally decoded to yield the observer's estimate (Fig. 3).

330 Originally, the model considers the Bayesian estimate as a direct reflection of participants'
331 reported estimate (Fig. 4a). With the extended model, however, we assume that participants'
332 perceptual estimate of heading $\theta(m)$ is mapped to their reported estimate $\hat{\theta}_r(m)$ via a linear
333 sensory-motor transformation, thus $\hat{\theta}_r(m) = \alpha_i \hat{\theta}(m)$ (Fig. 4b), where the scaling factor α_i depending
334 on the response range (see Methods).

335 We jointly fit this extended model to the data from individual participants in Experiment 3
336 across all three response conditions. We constrained the prior $p(\theta)$ on heading directions based on
337 the assumption that heading direction is efficiently represented in the brain. This assumption
338 predicts that the prior is inversely proportional to the discrimination threshold [20]. Specifically,
339 we used a smooth approximation of previously measured heading direction discrimination data [8]

to determine the prior on heading direction (see also [27]). The prior shows characteristic peaks for straight-ahead and straight-back directions (Fig 4c), in agreement with some measured behavioral statistics [26]. Importantly, in the interest of simplicity, we used this fixed prior for all model fits of individual participants' data. Furthermore, given the deterministic generation of the optic flow stimuli, we assume no external noise. This leaves us with only two free model parameters per participant: the overall sensory noise magnitude κ fixed across all response conditions, and the motor scaling α that is free for each response condition.

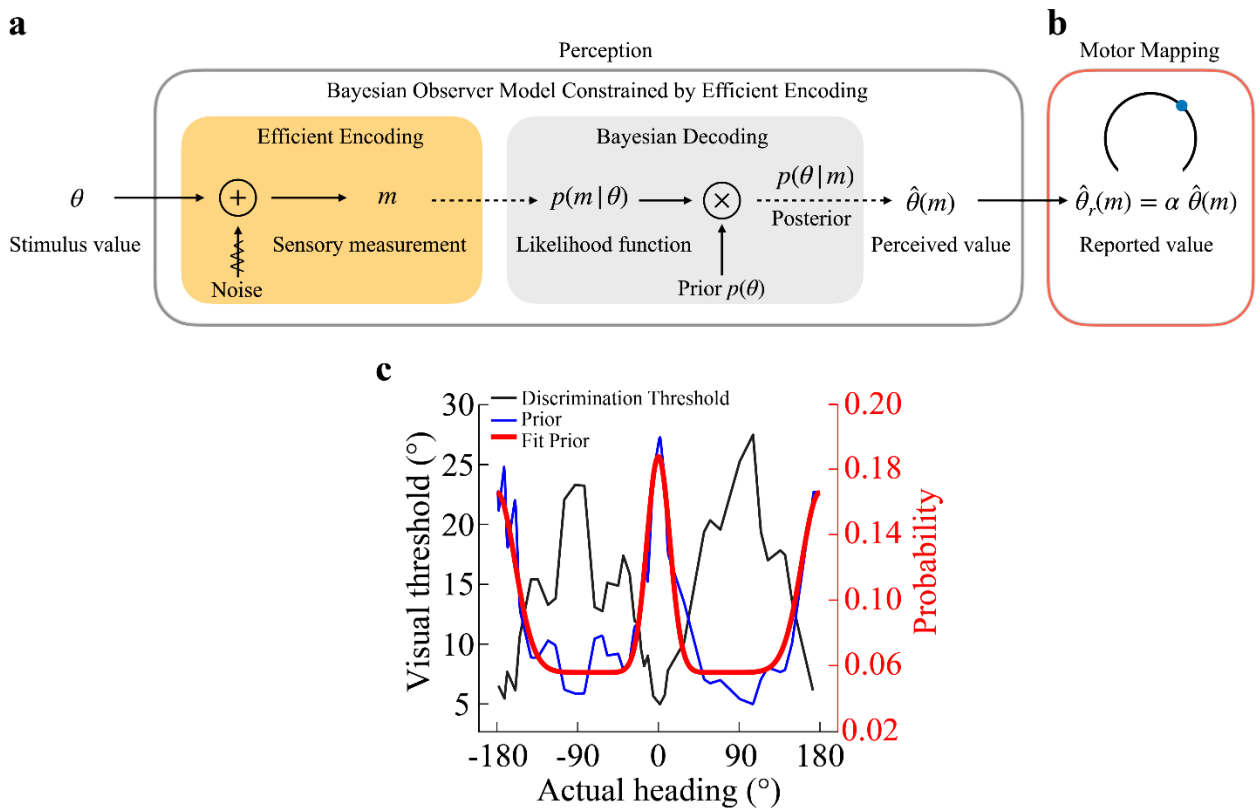

Fig. 4. Extended efficient Bayesian observer model. (a) The efficient Bayesian observer model as proposed by [19] assumes that the stimulus feature θ (e.g., heading direction) is first efficiently encoded in a sensory signal m before a Bayesian inference process computes an optimal estimate of the feature value $\hat{\theta}(m)$. (b) We extended the efficient Bayesian observer model by assuming a motor output stage that maps the perceptual estimate $\hat{\theta}(m)$ to the motor response that reflects the participants reports in the experiment $\theta_r(m)$.

We assume that this mapping is linear, thus $\theta_r(m)=\alpha_i\hat{\theta}(m)$ where is a scalar positive value that increases proportionally with the size of the response range. (c) Prior distribution for heading direction, $p(\theta)$. We estimate a single prior for all participants based on heading discrimination thresholds $D(\theta)$ previously measured by [8]. Under the efficient coding assumption, the prior is inversely proportional to $D(\theta)$ [20]. We smoothly approximate the experimentally determined prior with a two-peak von-Mises distribution, which captures the key characteristics of the natural distribution of heading directions encountered by humans during self-motion.

Note that the encoding precision, and thus the likelihood function, changes with heading direction but is precisely determined by the prior distribution (Fig. 4c) according to efficient coding. Because we assume the same approximation of the prior distribution for all participants, the likelihood functions of each participant are self-similar and only scaled by the individual sensory noise magnitude (see Methods).

Fig. 5 presents the results of our model fits. Fig. 5a shows the fit scaling factor α (group level, individual subjects, and average), which exhibits a positive correlation with the expansion of the response range. Fig. 5b shows the fit overall sensory noise level κ. Based on these two free parameters, our model generates detailed predictions for the bias and standard deviation of heading estimates, both at the group level (left panel of Fig. 5c) and individual level (right panel of Fig. 5c). These predictions demonstrate the model's ability to accurately represent the key characteristics of participants' data, both at the level of the average subject (Fig. 5d) as well as at the level of individual subjects (Fig. 6). Remarkably, the model effectively anticipates central biases (underestimation) when the response range is narrowest (80°). These biases transition to peripheral biases (overestimation) for broader response ranges (160° and 240°), with a discernible increase in bias corresponding to the enlargement of the response range. Similarly, the model

adeptly mirrors the overall characteristic of the standard deviation as a function of heading direction, showcasing a gradual magnitude increase with increasing response range while its pattern remains the same (Fig. 5e). This matches the observed pattern in participants' standard deviation (Fig. 5f and Fig. 6).

In conclusion, our results demonstrate that an extended efficient Bayesian observer model based on a naturalistic prior on heading direction can well account for participants heading estimation behavior (bias and standard deviation). The model assumes that participants' perceived heading direction is mapped to their reported heading direction via a linear sensorimotor transformation. The scaling factor monotonically depends on the specific response range provided to the participants in the experiment. Our results provide an intuitive, non-perceptual explanation for the apparently contrasting findings of both central (underestimation) and peripheral (overestimation) biases in heading estimation from optic flow.

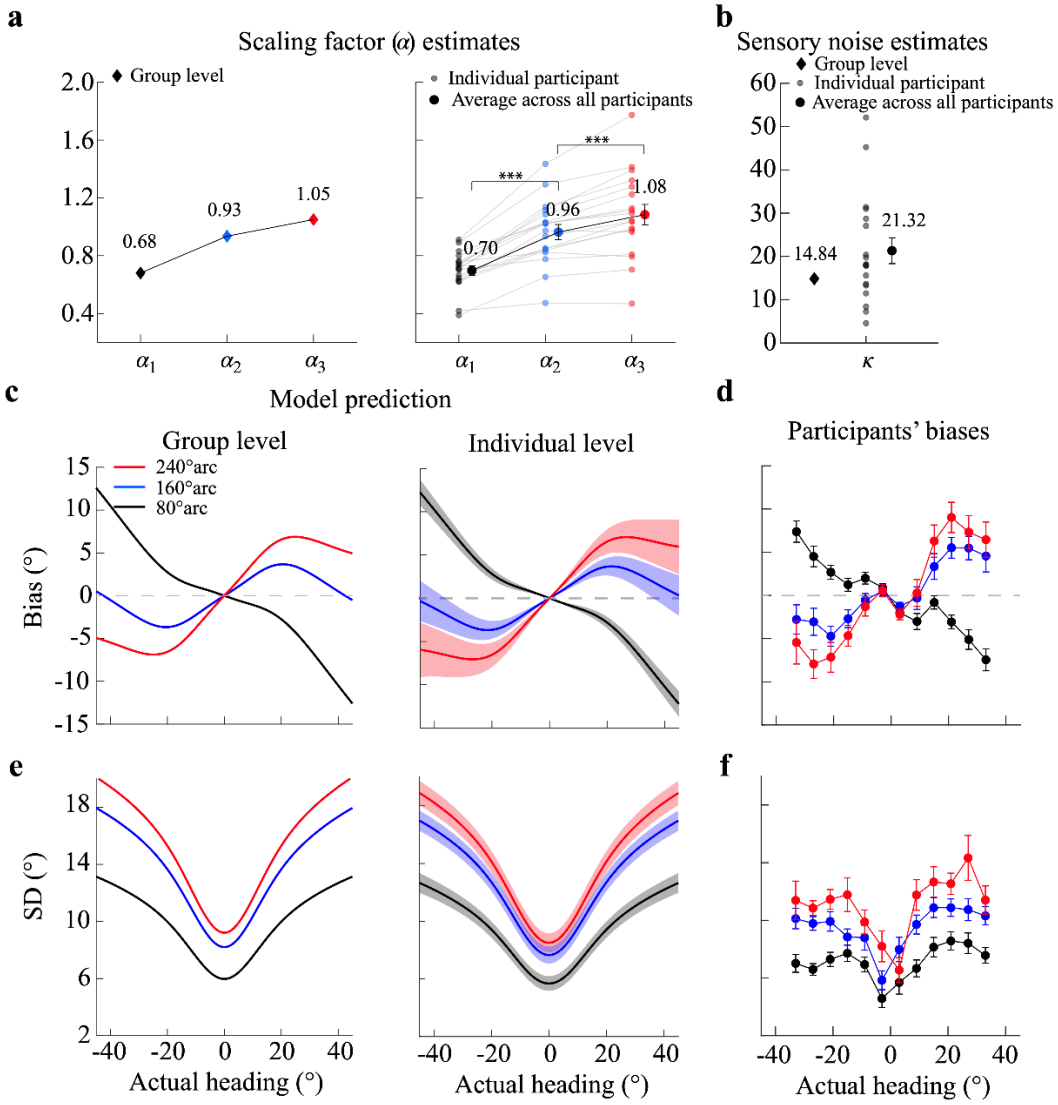

Fig. 5. Fit of the extended efficient Bayesian observer model to the data from Experiment 3. (a) Values of the scaling factor α from the group-level fit (left panel; combined data from all participants) and individual-level fits (right panel; fits to each participant's data). The right panel also shows the mean α values across participants for each response range condition. A repeated-measures ANOVA with Bonferroni-corrected post-hoc tests revealed that α significantly increases with the response range (***p<0.001). (b) Fit values of the sensory noise parameter κ (group-level and individual-level fits). (c, e) Model predictions for bias and standard deviation of heading estimates, respectively, based on the group-level (left panel) and individual-level (right panel) fits. Shaded areas represent the standard error across participants. (d, f) Mean

bias and standard deviation of heading estimates across the 18 participants in Experiment 3. Error bars indicate the standard error of the mean across participants.

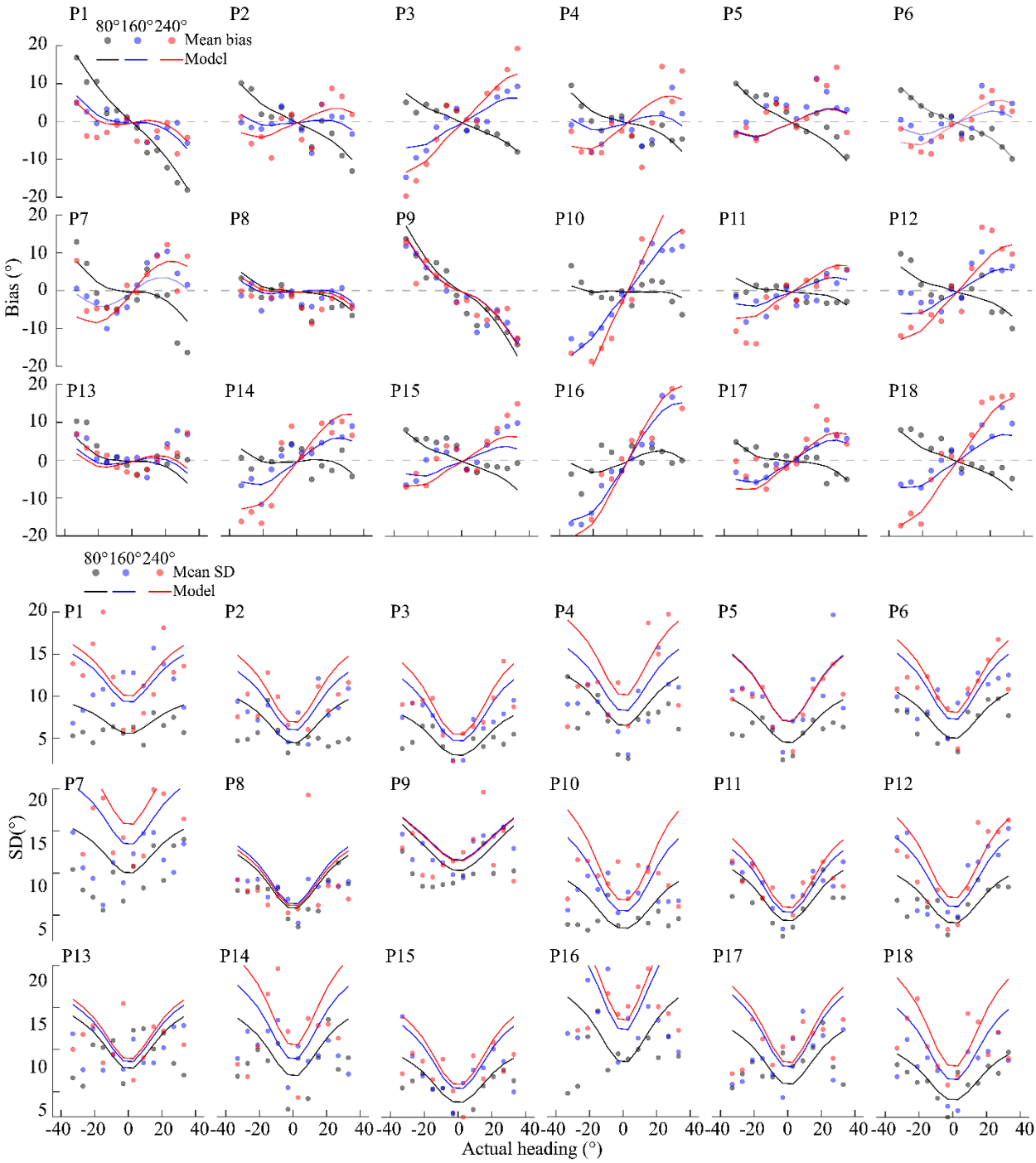

Fig. 6. Behavioral data and model fits for individual participants in Experiment 3, demonstrating the model's ability to capture individual-level patterns in heading estimation biases and variability.

Discussion

Our study demonstrates that the seemingly conflicting reports about human heading direction estimates can be fully explained by the influence of the response range in the psychophysical experiments. Specifically, participants' reported heading directions transitioned progressively from underestimation to overestimation with increasing response range (Fig 3). This transition can be well explained with an efficient Bayesian observer model [19], extended by a linear sensorimotor transformation between perceived and reported estimates that scales with the response range (Fig. 5a). We quantitatively validated this extended model. Our results provide a parsimonious and rational explanation for human heading perception, thereby reconciling seemingly conflicting previous reports of heading estimation biases. Our findings emphasize the significant role of motor control in shaping the reported estimates of stimulus features in psychophysical experiments, which has been often neglected in the past.

With only a few free parameters, our observer model is able to accurately express the large range of individual differences in subjects heading estimates, both in terms of bias and variance (Fig. 6). For our model, we assumed a fixed prior for heading direction based on the smooth approximation of previously recorded heading discrimination data [8]. According to the efficient coding assumption of the model, the prior is defined as being proportional to the inverse of the discrimination threshold function [20]. Although this is an indirect way of determining the prior, previous studies have shown that it faithfully captures the statistical prior in the visual environment for other stimulus variables such as local orientation [28] and visual motion [29]. Furthermore, preliminary data on the actual heading direction statistics of freely behaving human observers seem to support the predominance of straight-ahead heading [26]. Future studies are necessary to

425 determine in more detail the exact shape of the prior distribution by using careful measurements
426 of the natural statistics of human heading behavior.

427 Such statistical measurements of the natural prior of human heading directions will also help
428 to explain another interesting characteristic of our data. Although our observer model overall well
429 explains the data, there are slight but systematic deviations between data and model predictions,
430 especially with regard to the bias pattern around straight-ahead heading (0 degrees). Under all
431 response conditions, participants' bias curves are non-monotonic (i.e., they show a "wiggle") in
432 the range of 0-15 degree heading direction, which is not accounted for by the model using the
433 current prior. However, a prior with non-monotonic fall-off (i.e. with some side peaks close to
434 straight-ahead heading) likely would capture this behavior. An alternative explanation is that these
435 non-monotonic bias patterns are not due to a non-monotonic prior distribution, but may be the
436 signature of a categorical influence in participants heading estimates [30].

437 Our model makes clear predictions with regard to stimulus (external) and sensory (internal)
438 noise (Fig. 4a). Due to the efficient coding assumption, the two noise sources differentially affect
439 the perceptual estimate [19]. In our experiments, the optic flow pattern was fully coherent with
440 each simulated heading direction and thus the stimulus noise was zero. Furthermore, dot densities
441 and contrasts, as well as stimulus presentation times were fixed, thus sensory noise was assumed
442 to be constant. Our model predicts that adding stimulus noise (e.g., by reducing the fraction of dots
443 with coherent optic flow motion) would lead to an increase in central bias (i.e., a decrease in
444 peripheral bias, respectively), while an increase in sensory noise (e.g., by reducing the presentation
445 time of the flow pattern) would decrease central bias (i.e., increase peripheral bias, respectively).
446 Note, our model provides these quantitative predictions at the level of both, bias and variance

447 across the entire heading direction range. Future studies employing targeted psychophysical
448 experiments will be able to specifically test those predictions and further validate the model.

449 It is important to note that in our experiments, participants did not receive visual feedback
450 about the correct heading direction after reporting their estimates. This was a deliberate choice in
451 order to be consistent with the experimental designs of previous studies. Without feedback, it is
452 likely that participants in these all studies used their experience of the response range to calibrate
453 their motor responses with which they indicated their perceived heading estimates. This would
454 explain the monotonic scaling of the estimates with the size of the response range in our study.
455 Several studies have shown that real-time feedback can improve our visual perception [5, 31-33].
456 Thus, it is an interesting open question to ask to what degree feedback will reduce or even eliminate
457 the effects of the response range on heading estimation. Based on our model, we predict that with
458 feedback, participants will be able to quickly recalibrate and substantially reduce the observed bias
459 because the biases are mostly attributed to the linear sensorimotor mapping. We expect that the
460 remaining biases will then mainly reflect only the inductive biases that are intrinsic to the Bayesian
461 inference process due to the prior and the non-homogeneous, efficient encoding.

462 In conclusion, our study successfully demonstrates that the contrasting findings of
463 underestimation and overestimation biases reported in several previous studies can be fully
464 explained by the different sizes of response range used in these different studies. We show that
465 participants' reported estimates under different response range conditions are quantitatively
466 accounted for by an extended efficient Bayesian observer model that incorporates a linear (motor)
467 mapping between perceived and reported estimates. This suggests that human heading perception
468 follows efficient Bayesian inference and is not dependent on the specific response characteristics
469 of a psychophysical experiment; the observed differences in participants' reported estimates cam

be solely attributed to the difference in mapping from percept to probe response. As such, our model is the first that provides a unifying account of a wide range of heading estimation datasets. Our findings contribute to a more comprehensive understanding of human perception and have implications for the design of navigational aids and virtual reality systems.

Data and code

All data and modeling codes have been deposited on OSF:
https://osf.io/t47v6/?view_only=659d4bac8e4344f996eb8a51eb236d55

Funding

This study was supported by National Natural Science Foundation of China, China (No. 32200842) to Qi Sun and in part by the University of Pennsylvania (to AAS).

Acknowledgement

We thank Bao-Yin Zhang and Lin-Zhe Zhan for collecting the data and doing the pilot data analysis.

References

1. Appelle, S. Perception and discrimination as function of stimulus orientation. Psychol Bull. 1972; 78, 266–278. https://doi.org/10.1037/ h0033117
2. Olkkonen M, McCarthy PF, Allred SR. The central tendency bias in color perception: Effects of internal and external noise. J Vis. 2014; 14(11):5. http://www.journalofvision.org/content/14/11/5

3. De Gardelle V, Kouider S, Sackur J. An oblique illusion modulated by visibility: Non-monotonic sensory integration in orientation processing. 2010; J Vis. 10(10):6. http://www.journalofvision.org/content/10/10/6
4. Taylor R, Bays PM. Efficient coding in visual working memory accounts for stimulus-specific variations in recall. Neurosci J. 2018; 38(32):7132–7142. https://doi.org/10.1523/JNEUROSCI.1018-18.2018
5. Noel JP, Zhang LQ, Stocker AA, Angelaki DE. Individuals with autism spectrum disorder have altered visual encoding capacity. PLoS Biol. 2021; 19(5):e3001215. https://doi.org/10.1371/journal.pbio.3001215
6. Crane BT. Direction specific biases in human visual and vestibular heading perception. PloS One. 2012; 7(12):e51383. https://doi.org/10.1371/journal.pone.0051383
7. Cuturi LF, MacNeilage, PR. Systematic biases in human heading estimation. PloS One. 2013; 8(2):e56862. https://doi.org/10.1371/annotation/38466452-ba14-4357-b640-5582550bb3dd
8. Gu Y, Fetsch CR, Adeyemo B, DeAngelis GC, Angelaki DE. Decoding of MSTd population activity accounts for variations in the precision of heading perception. Neuron. 2010; 66(4):596-609. doi: 10.1016/j.neuron.2010.04.026.
9. D'Avossa G, Kersten D. Evidence in human subjects for independent coding of azimuth and elevation for direction of heading from optic flow. Vis Res. 1996; 36(18):2915-2924. https://doi.org/10.1016/0042-6989(96)00010-7
10. Sun Q, Zhan LZ, You FH, Dong XF. Attention affects the perception of self-motion direction from optic flow. iScience. 2024; 27:109373. https://doi.org/10.1016/j.isci.2024.109373

11. Sun Q, Zhan LZ, Zhang BY, Jia S, Gong XM. Heading perception from optic flow occurs at both perceptual representation and working memory stages with EEG evidence. Vis Res. 2023; 208:108235. https://doi.org/10.1016/j.visres.2023.108235

12. Wang XY, Gong XM, Sun Q, Li X. Attractive effects of previous form information on heading estimation from optic flow occur at perceptual stage. J Vis. 2022; 22(12):18. https://doi.org/10.1167/jov.22.12.18

13. Warren WH, Kurtz KJ. The role of central and peripheral vision in perceiving the direction of self-motion. Percept Psychophys. 1992; 51(5), 443-454.

14. Warren Jr WH, Saunders JA. Perceiving heading in the presence of moving objects. Perception, 1995; 24(3):315-331. https://doi.org/10.1068/p24031

15. Xu LH, Sun Q, Zhang B, Li X. Attractive serial dependence in heading perception from optic flow occurs at the perceptual and postperceptual stages. J Vis. 2022; 22(12):11. https://doi.org/10.1167/jov.22.12.11

16. Crane BT. Human visual and vestibular heading perception in the vertical planes. JARO. 2014; 15:87-102. doi: 10.1007/s10162-013-0423-y

17. Gibson JJ. The perception of the visual world. Boston, MA: Houghton Mifflin; 1950.

18. Wei XX., Stocker AA. Efficient coding provides a direct link between prior and likelihood in perceptual Bayesian inference. Adv Neural Inf Process Syst. 2012; 25:1-9.

19. Wei XX, Stocker, AA. A Bayesian observer model constrained by efficient coding can explain 'anti-Bayesian' percepts. 2015; Nat Neurosci. 18(10):1509-1517. https://doi.org/10.1038/nn.4105

20. Wei XX, Stocker AA. Lawful relation between perceptual bias and discriminability. PNAS. 2017; 114(38):10244-10249. https://doi.org/10.1073/pnas.1619153114

21. Attneave F. Some informational aspects of visual perception. Psychol Rev. 1954; 61(3):183-193. https://doi.org/10.1037/h0054663

22. Barlow HB. Possible principles underlying the transformation of sensory messages. Sensory Communication. 1961; 1(01):217-233

23. Geisler WS, Kersten D. Illusions, perception and Bayes. Nat Neurosci. 2002; 5(6):508-510. https://doi.org/10.1038/nn0602-508

24. Knill DC, Richards W. Perception as Bayesian inference. Cambridge University Press; 1996.

25. Weiss Y, Simoncelli E P, Adelson EH. Motion illusions as optimal percepts. Nat Neurosci. 2022; 5(6):598-604. https://doi.org/10.1038/nn0602-858

26. Sinnott C, MacNeilage P. Statistical characterization of heading stimuli in natural environments using SLAM. J Vis. 2019; 19(8):53. https://doi.org/10.1167/19.8.53

27. Crowell JA., Banks, MS. Perceiving heading with different retinal regions and types of optic flow. Percept Psychophys. 1993; 53(3):325-337. https://doi.org/10.3758/BF03205187

28. Ganguli D, Simoncelli EP. (2014). Efficient sensory encoding and Bayesian inference with heterogeneous neural populations. Neural Comput. 2014; 26(10), 2103-2134. DOI: 10.1162/NECO_a_00638

29. Zhang LQ, Stocker AA. Prior expectations in visual speed perception predict encoding characteristics of neurons in area MT. J Neurosci. 2022; 42(14), 2951-2962. https://doi.org/10.1523/JNEUROSCI.1920-21.2022

30. Mao J, Stocker AA. Sensory perception is a holistic inference process. Psychol Rev. 2024; Advance online first. https://dx.doi.org/10.1037/rev0000457

31. Alenezi HM, Bindemann M. The effect of feedback on face-matching accuracy. Appl Cogn Psychol. 2013; 27(6):735-753. https://doi.org/10.1002/acp.2968

32. Attar N, Wu CC, & Pomplun M. The effect of immediate accuracy feedback in a multiple-target visual search task. In Proceedings of the Annual Meeting of the Cognitive Science Society. 2014; 36(36):1868-1873.

33. Bjasch D, Bockisch CJ, Straumann D, Tarnutzer AA. Differential effects of visual feedback on subjective visual vertical accuracy and precision. PLoS One. 2021; 7(11):e49311. https://doi.org/10.1371/journal.pone.0049311

Supporting Information

S1 Movie. Optic flow with constant speed.

S2 Movie. Optic flow with variable speed.

Click the link to watch the two movies:
https://osf.io/x57w6/?view_only=a3603f0a89ba4280ace258e4876385dc